Out-of-equilibrium dynamics in the cytoskeleton of the living cell

Guillaume Lenormand, Predrag Bursac, James P. Butler, and Jeffrey J. Fredberg
Molecular and Integrative Physiological Sciences, Department of Environmental Health, Harvard School of Public Health, 665 Huntington Avenue, Boston, Massachusetts 02115, USA

(Received 23 February 2007; revised manuscript received 9 July 2007; published 1 October 2007)

We report here measurements of rheological properties of the human airway smooth muscle cell using forced nanoscale motions of Arg-Gly-Asp RGD-coated microbeads tightly bound to the cytoskeleton. With changes of forcing amplitude, the storage modulus showed small but systematic nonlinearities, especially after treatment with a contractile agonist. In a dose-dependent manner, a large oscillatory shear applied from a few seconds up to 400 s caused the cytoskeleton matrix to soften, a behavior comparable to physical rejuvenation observed in certain inert soft materials; the stiffness remained constant for as long as the large oscillatory shear was maintained, but suddenly fell with shear cessation. Stiffness then followed a slow scale-free recovery, a phenomenon comparable to physical aging. However, acetylated low-density lipoprotein acLDL-coated microbeads, which connect mainly to scavenger receptors, did not show similar out-of-equilibrium behaviors. Taken together, these data demonstrate in the cytoskeleton of the living cell behaviors with all the same signatures as that of soft inert condensed systems. This unexpected intersection of condensed matter physics and cytoskeletal biology suggests that trapping, intermittency, and approach to kinetic arrest represent central mesoscale features linking underlying molecular events to integrative cellular functions.

DOI: 10.1103/PhysRevE.76.041901 PACS number(s): 87.16.Ka, 83.60.Rs, 83.85.Cg, 87.17.−d

I. INTRODUCTION

Mechanical properties of the living cell are largely determined by its cytoskeleton (CSK), a complex biopolymer network consisting of filamentous actin, microtubules, and intermediate filaments, many of which are associated with crosslinkers, motor proteins, and other regulatory proteins. In recent years, the physical environment of a living cell, such as forces applied to it or the stiffness of its surrounding material, has been shown to influence biological functions [1–3]. In this paper, we focus on how a mechanical shear affects physical properties of the cytoskeletal network. Although the literature emphasizes stiffening [4–9], there is now clear evidence that, when submitted to shear, some biological systems display a prompt softening, which is then followed by stiffening [10–13].

In addressing the effects of physical forces upon cell mechanical properties, we have suggested previously that the CSK of a living cell exhibits slow "glassy" dynamics similar to those observed in soft condensed matter [11,13,14]. In glassy systems, a particle can become trapped by interactions with its surrounding neighbors [15,16]. Because these neighbors act as a cage, particle motions are localized most of the time, although occasionally a particle escapes its trap and thus causes the local configuration to rearrange. With time, however, the system evolves into configurations that are more and more stable, but more slowly than any exponential process; i.e., the system stiffens with time. Slowly evolving dynamics of this kind is called physical aging [17,18]. In such systems, applying a sufficiently large oscillatory shear can provide an additional energy source that can overcome energy barriers and drive structural rearrangements. As a consequence, material properties return to their earlier values. In this way aging is reversed and the system softens. This phenomenon is called physical rejuvenation [17,18].

In this paper, we show that a large oscillatory shear softened the CSK, a behavior similar to physical rejuvenation observed in inert glassy materials. This softening was followed by a slow scale-free recovery, a behavior similar to physical aging. After reviewing artifacts that might have been induced by the experimental approach, we go on to discuss insights that these findings provide concerning material properties of the living scell. Finally, we show that these new data further strengthen the analogy between the behavior of the CSK and that of soft condensed matter, including soft glassy materials (SGMs). This paper provides new data extending a previous short communication from our group [13].

II. MATERIALS AND METHODS

Mechanical properties were measured using magnetic twisting cytometry with optical detection of microbead motion. Optical magnetic twisting cytometry (OMTC) can be thought of as a microrheometer in which the cell is deformed between a plate at the cell base (the cell culture dish upon which the cell is adherent) and a magnetic microbead partially embedded into the cell surface (Fig. 1). Microbead coating, cell preparation, the experimental setup, and mechanical measurements used in this paper have been reported in detail elsewhere [13,19] and are briefly described below; methodological limitations are reviewed in the Discussion.

A. Microbead and cell preparation

Ferrimagnetic microbeads (4.2 μm in diameter) were produced in our laboratory, and then coated using one of two different ligands: either acetylated low-density lipoprotein (acLDL) or a peptide containing the sequence Arg-Gly-Asp (RGD—exact sequence: Ac-Gly-DArg-Gly-Asp-Ser-Pro-Ala-Ser-Pro = Ala-Ser-Ser-Lys-Gly-Gly-Gly-Gly-Ser-DArg-Leu-Leu-Leu-Leu-Leu-Leu-DArg-NH_2). Each ligand was adsorbed onto the microbead surface (150 μg ligand/mg mi-

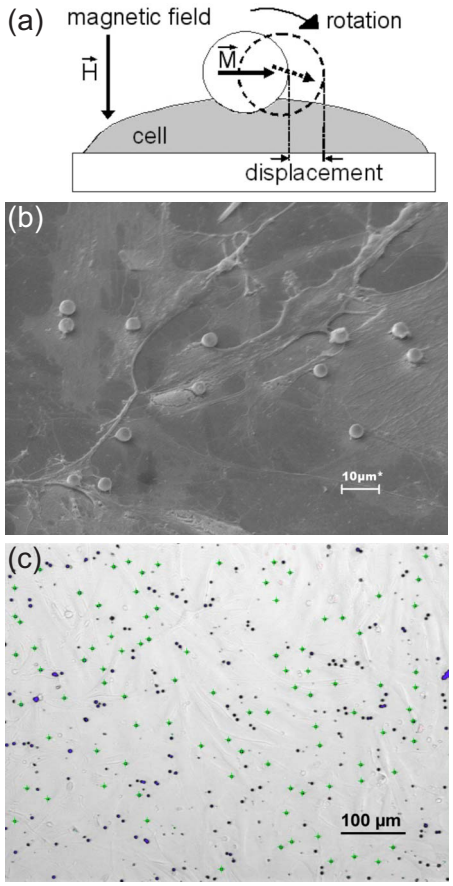

FIG. 1. (Color online) Optical magnetic twisting cytometry. (a) Magnetized microbeads acquired a magnetic moment $\vec{M}$. A magnetic twisting field $\vec{H}$ induced a mechanical torque on each microbead and caused the microbead to rotate and translate. $\vec{M}$ denotes the direction of the microbead's magnetic moment before (plain line) and after (dotted line) twisting. (b) Scanning electron micrograph (EM) of RGD-coated microbeads firmly attached to the surface of HASM cells (EM stage was tilted by 45°). (c) Bright field image of HASM cells with magnetic microbeads (black dots) during measurements. Microbeads marked with a green cross have been recognized by the algorithm.

crobeads) by overnight incubation at 4 °C in carbonate buffer (pH 9.4). The microbead coated with AcLDL binds to low-density lipoprotein receptors, a nonadhesion scavenger receptor. The microbead coated with RGD, by contrast, attaches to the human airway smooth muscle (HASM) cell via integrin receptors, mainly through β_1 subunits [20]. The integrins then cluster in localized attachment domains and assemble into adhesion complexes [21]. As addressed in the Discussion, data suggest that such a microbead is strongly anchored to the CSK.

HASM cells in passages 6–7 were serum deprived for 36 h; serum deprivation arrests the cell cycle in the G_1/G_0 phases. Plastic wells (6.4 mm, 96-well Removawells, Immunlon, IL) were coated with collagen I at a density of 500 ng/cm^2 for at least 12 h. Cells were harvested with trypsin and incubated overnight in collagen-coated wells at confluence (~20 000 cells/well). Prior to each measurement, approximately 10 000 microbeads were added to an individual well and incubated for 20 min, leading to an average of one microbead per living cell. The well was then rinsed twice with a serum-free medium at room temperature to remove unbound microbeads. Once mounted on the microscope stage, the microbeads were magnetized twice and an experimental protocol began. All measurements were performed at room temperature. So that the loading history was identical between measurements, each well was tested only once, and within a group of experiments, wells were submitted to the exact same preparation history.

B. Microbead twisting and measurement of microbead motion

A pair of magnetizing coils and a pair of twisting coils were mounted on the stage of an inverted microscope. The well was placed on the microscope stage, and the microbeads were magnetized horizontally by two consecutive magnetic pulses (~0.1 T for ~0.1 ms) using the magnetizing coils [Fig. 1(a)]. Furthermore microbeads were remagnetized 5 s before applying the large oscillatory shear and before each step torque. A vertical magnetic field $\vec{H}$, applied by the twisting coils, induced a mechanical torque on each microbead, and caused both a rotation and a lateral displacement of the microbeads [22]. The mechanical torque per microbead volume T is given by $T=cH\cos\theta$, where c is the microbead magnetic constant ($c=2.1$ Pa per gauss), and θ is the angle of microbead rotation. Because θ was small, we could ignore the cos θ term when computing the specific torque T from the twisting field [22]. A progressive scan, triggerable black-and-white CCD camera with pixel-clock synchronization (JAI CV-M10, Glostrup, Denmark) was attached to the camera side port of the microscope. Image acquisition was phase locked to the twisting field. In any given well, the individual displacements of approximately a hundred microbeads were recorded simultaneously using an intensity-weighted center-of-mass algorithm [Fig. 1(c)]. Moreover, beads that were within two bead diameters were not analyzed to avoid correlated motions of adjacent beads. The accuracy in the microbead position was 10 nm (rms); the exposure time was 0.1 ms.

C. Complex elastic modulus

Sinusoidal forcing at frequency f was used to measure a storage modulus $g'(f)$, and a loss modulus $g''(f)$ [14,23]. Measurements were performed over four decades in frequency, from 0.1 Hz to 1 kHz. Sixteen images were acquired during a twisting cycle, and heterodyning (a stroboscopic technique) was used at frequencies above 1 Hz. The complex elastic modulus $g^*(f)$ was defined by $g^*(f)=\tilde{T}(f)/\tilde{d}(f)$, where $\tilde{T}$ is the Fourier transform of the mechanical torque per microbead volume, $\tilde{d}$ is the Fourier transform of the resulting microbead displacement, and $g^*(f)=g'(f)+ig''(f)$ with $i^2=-1$. This complex elastic modulus has dimensions of Pa/nm and can be transformed to the conventional complex elastic modulus $G^*(f)$ (with units of Pa) by a geometric factor α through the relationship $G^*(f)=\alpha g^*(f)$. The geometric

factor α has been evaluated using a finite element model of cell deformation [22], and depends mainly on the cell height and on the degree of microbead embedding. Assuming 10% of the microbead diameter embedded in a cell 5 μm high sets α to 6.8 μm. The complex elastic modulus $g^*(f)$ was measured for each single microbead from its individual displacement, and we report a median value of $g^*(f)$ calculated over a large number of microbeads n. This number is usually greater than 400 and is given in the figure legends.

D. Creep function

To measure the creep function [24], a constant magnetic field was applied causing the microbeads to rotate and translate; the displacement $d(t)$ of each microbead at times t was recorded. We defined the creep function as $j(t)=d(t)/T_0$, T_0 being the constant specific torque. This creep function has dimensions of nm/Pa and can be transformed to the conventional creep function $J(t)$ (with units of Pa^{-1}) using the same geometric factor α such as $J(t)=j(t)/\alpha$. For RGD-coated microbeads, the creep function was measured applying a small step torque of 42 Pa; for acLDL-coated microbeads, the applied torque was 3 Pa. Microbeads that moved less than 20 nm after 3 s of torque application were considered to have fallen below our noise floor, and were discarded; this corresponded to fewer than 20% of the microbeads. Because we use median statistics, whether these microbeads were included or rejected had at most only slight influence on the phenomena reported. Furthermore, with RGD-coated microbeads, a torque of 42 Pa has been shown not to induce significant changes in mechanical properties, whereas one above 80 Pa did [13]. Note that the creep function $j(t)$ was measured for each single microbead from its individual displacement, and we report a median value of $j(t)$ calculated over a large number of microbeads n. This number is usually greater than 400 and is given in the figure legends.

E. Cytoskeleton modulation

The CSK mechanical properties were modulated by treatment of the cell with dibutyryl adenosine 3′,5′-cyclic monophosphate (DBcAMP, decreases cell contractility, 1 mM), and histamine (increases cell contractility, 100 μM). DBcAMP and histamine were reconstituted in sterile distilled water at 0.1 M. Phenylarsine oxide (PAO, 5 nM), a tyrosine phosphatase inhibitor, was prepared in sterile DMSO. On the day of experiments, all reagents were diluted to final concentrations in serum-free media, yielding $<0.1\%$ DMSO in final volume.

F. Reagents

Tissue culture reagents and drugs used in this study were obtained from Sigma (St. Louis, MO, USA), with the following exceptions: Trypsin-ETDA solution, which was purchased from Gibco (Grand Island, NY), type I rat tail collagen (Vitrogen Collagen) from Cohesion Technologies (Palo Alto, CA), RGD peptide (Peptide 2000) from Telios Pharmaceuticals (San Diego, CA), AcLDL from Biomedical Technologies (Stoughton, MA).

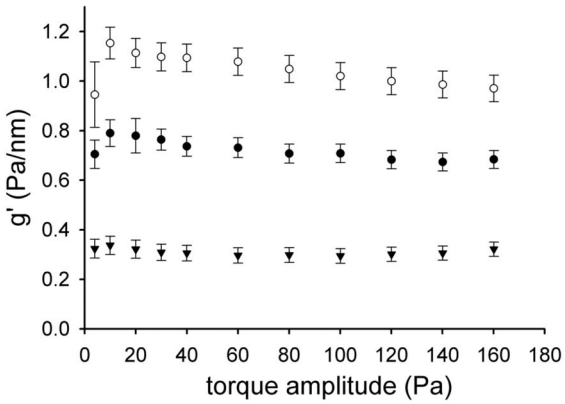

FIG. 2. Storage modulus g' of HASM cells versus applied specific torque T (twisting frequency of 0.75 Hz), at baseline condition (●, $n=595$ microbeads), and after treatment with histamine (○, $n=445$ microbeads) and DBcAMP (▼, $n=834$ microbeads). With changes of forcing amplitude, g' showed small but systematic nonlinearities, especially after treatment with histamine (a contractile agonist). Error bars indicate ± standard error.

G. Statistics

We used a t test to determine whether changes were statistically significant ($p<0.001$).

III. RESULTS

A. Dependence of the complex modulus upon torque amplitude

We investigated nonlinearities by measuring the dependence of storage g' and loss g'' moduli upon the amplitude of the specific torque oscillation, which was varied over a range approaching 40-fold (Fig. 2). Measurements were performed as the torque amplitude was first increased then decreased. No significant differences were observed between the two measurements, thus g' was independent of the sequence of the applied torques. As the amplitude was progressively increased, g' first increased, peaked when specific torque was about 10 Pa, and as the amplitude was further increased, g' decreased only slightly (Fig. 2). When cells were contracted with histamine, g' increased and reached a steady state within minutes [23]. When the specific torque amplitude was then progressively increased, g' peaked when specific torque was about 10 Pa, and slightly decreased for higher torques. This amplitude dependence of g' was accentuated compared to baseline conditions, but remained quite small. When cells were relaxed with DBcAMP, g' decreased, and reached a steady state within minutes [23]. As the amplitude of the oscillatory torque was subsequently increased, g' remained constant, implying no amplitude dependence. In each of these cases, g'' showed similar behavior but with absolute values approximately 10 times smaller (data not shown). With increasing torque amplitude, changes in g' and g'' were weak, and at first approximation, the system could be regarded as linear.

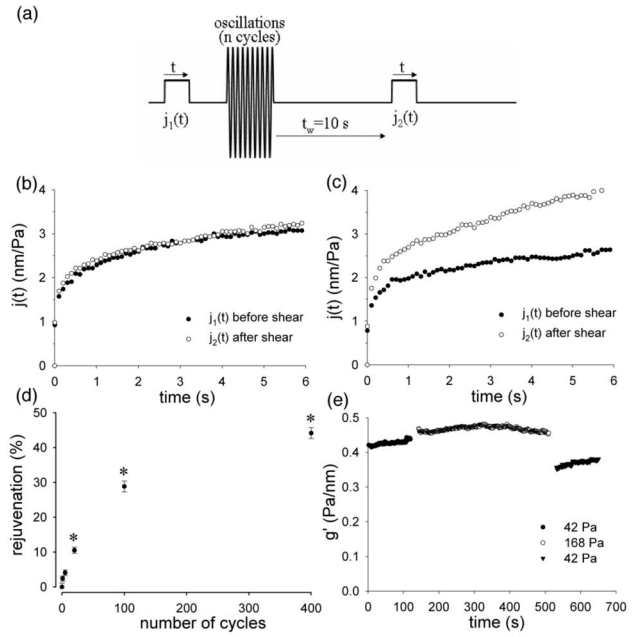

FIG. 3. Rejuvenation: influence of a large oscillatory shear on mechanical properties. (a) Stress history used for Figs. 3(b)–3(d). A small step torque (42 Pa) was first applied to measure the creep function $j_1(t)$. The CSK was then sheared by applying a large oscillatory torque (1 Hz, 100 Pa); the number of oscillations varied from 0 to 400. A second small step torque was applied 10 s after the end of the oscillations to measure $j_2(t)$. (b) When no shear was applied, no difference was observed between the creep functions $j_1(t)$ and $j_2(t)$; the stiffness was identical. (c) When a large shear was applied for 400 s, the creep function $j_2(t)$ was increased compared to $j_1(t)$, indicating that the large oscillatory shear had softened the CSK. (d) Rejuvenation was defined as a percent change between $j_1(t=3\ \mathrm{s})$ and $j_2(t=3\ \mathrm{s})$. As the number of oscillations increased, creep measured upon cessation of the oscillations increased as well, indicating partial rejuvenation. * denotes a change statistically significant ($p<0.001$). (e) Storage modulus g' measured by applying a small specific torque of 42 Pa (●), then a large torque of 168 Pa (○), and a small torque again (▼) (twisting frequency 0.75 Hz). The stiffness remained nearly constant for as long as the large oscillatory shear was maintained, but fell by 28% with cessation of this large shear (median values over $n>400$ microbeads).

B. Physical rejuvenation

We then turned to changes in mechanical properties induced by a large oscillatory shear. To do this we measured the creep functions before and after application of a large oscillatory torque, which we called $j_1(t)$ and $j_2(t)$, respectively [Fig. 3(a)]. For each measurement, the amplitude of the large oscillatory torque remained constant (100 Pa at 1 Hz), but the number of cycles was varied. We expressed the change between $j_1(t)$ and $j_2(t)$, both taken at $t=3$ s (an arbitrary value), as a percent change, and called this a rejuvenation response. When no shear was applied, no difference was observed between $j_1(t)$ and $j_2(t)$; the stiffness was identical [Fig. 3(b)]. In contrast, when a large shear was applied for 400 s, $j_2(t)$ measured subsequently increased compared to $j_1(t)$ [Fig. 3(c)]; for an identical applied torque

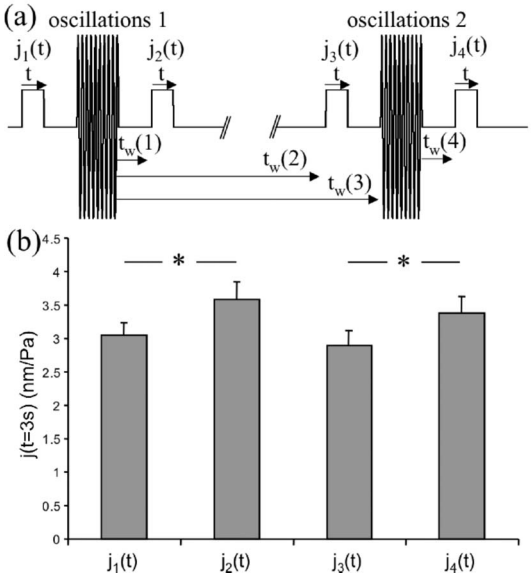

FIG. 4. Rejuvenation: influence of a second oscillatory shear. (a) Stress history. A first step torque was applied, and then the matrix was sheared (1 Hz, 20 cycles, 100 Pa). A second step was applied at $t_w(1)=10$ s after the end of the oscillations. At $t_w(2)=400$ s, a third step was applied. At $t_w(3)=430$ s, the matrix was sheared a second time (1 Hz, 20 cycles, 100 Pa), and a fourth step was applied at $t_w(4)=10$ s after the end of the second oscillation. (b) Median values and standard error for each of the four creep functions at $t=3$ s ($n=1661$ microbeads). j_1 gives the baseline condition. j_2 following the large shear is consistent with partial rejuvenation. j_3 showed a decrease in stiffness consistent with aging. j_4 revealed that the second oscillations reversed aging and brought back the mechanical properties to 92% of j_2. * denotes a change statistically significant ($p<0.001$).

the microbeads moved more, indicating that the large oscillatory shear softened the CSK. As the number of applied torque cycles increased, rejuvenation increased in a dose-dependent manner [Fig. 3(d)]; the CSK became progressively softer as the number of cycles applied previously was increased.

To further explore the influence of large shear on mechanical properties, we measured g' and g'' before, during, and after a large oscillatory shear [Fig. 3(e)]. The torque was turned off for 20 s between each measurement during which microbeads were remagnetized. During the first phase of the measurement (small torque of 42 Pa at 0.75 Hz), g' remained nearly constant [Fig. 3(e)]. During the second phase (large torque of 168 Pa), g' was not much different, reflecting the insensitivity of g' to torque amplitude as described above. Interestingly, the stiffness remained nearly constant for as long as this oscillatory shear was maintained. It was only with cessation of this large shear that g' rapidly fell.

The ability of shear to rejuvenate the system was further tested by applying two consecutive large oscillatory torques [Fig. 4(a)]. After the first large oscillatory shear, $j_2(t)$ was about 20% higher than $j_1(t)$; the oscillatory shear softened the cell, indicative of rejuvenation [Fig. 4(b)]. During the waiting time of 400 s, $j_3(t)$ decreased compared to $j_2(t)$; the

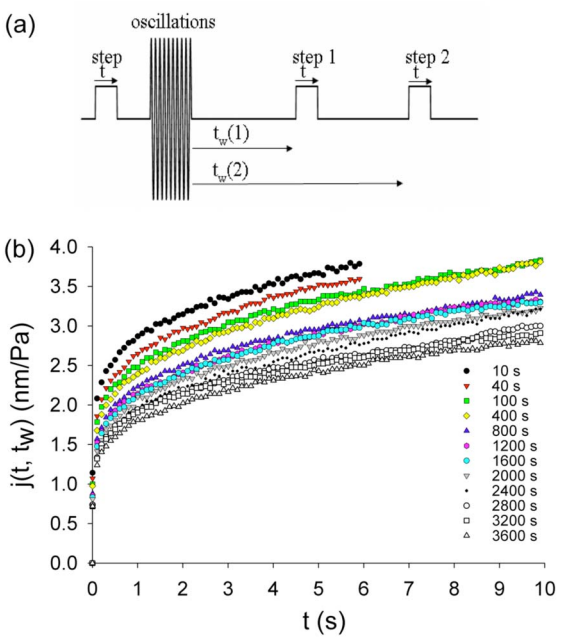

FIG. 5. (Color online) Aging: changes in the creep functions $j(t,t_w)$ at different waiting times t_w. (a) Stress history. Creep functions were measured by applying a small step torque before and after application of a large oscillatory shear. The waiting time t_w was defined upon cessation of the large shear. (b) Median values ($n=1684$ microbeads) of creep functions at different t_w, ranging from 10 to 3600 s (top to bottom, respectively). The stiffness of the CSK increased with the waiting time, a behavior consistent with physical aging.

cell stiffened, indicative of aging (see below). A second oscillatory shear was then applied; $j_4(t)$ measured upon cessation of this second shear was increased, and was brought back to 92% of $j_2(t)$. These findings confirmed that a large shear rejuvenated the CSK and reversed aging.

C. Physical aging

We now turn to the evolution of mechanical properties following the large shear. Microbeads were first incubated on cells for 20 min. Then, for reasons explained in the Discussion ("Evolution of mechanical properties"), the cell well was left at rest for 1 h. Creep functions were measured before and at different waiting times t_w, after application of a large oscillatory torque [Fig. 5(a)]. These creep functions become a function of two times: the time t, elapsed since the imposition of the step torque, and the waiting time t_w, elapsed since the end of the large oscillatory torque.

As previously reported [19], each creep function $j(t,t_w)$, increased with t as a weak power law, i.e., $j(t)=j_0t^{x-1}$ [Fig. 5(b)]. After application of the large oscillatory shear, j_0 decreased systematically as the waiting time was increased, whereas x increased slightly from 1.15 to 1.18 within the first 400 s, and remained constant and equal to 1.179 ± 0.009 for longer waiting times. The creep functions decreased as t_w increased; thus the CSK stiffened as the waiting time increased, a behavior similar to that observed in certain soft

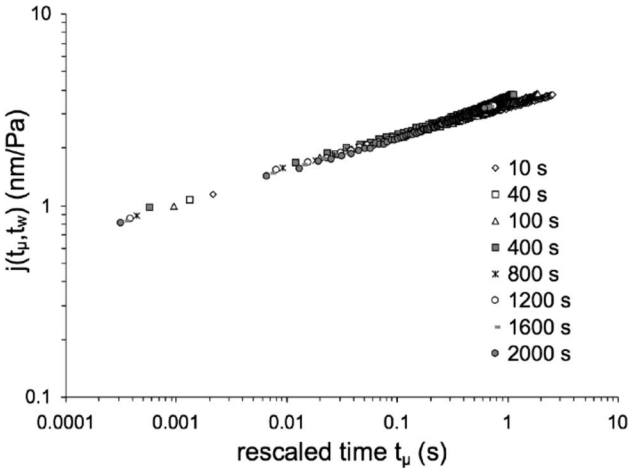

FIG. 6. Collapse of the creep functions. When plotted versus a rescaled time t_μ, defined as $t_\mu=t/(t_w)^\mu$, all creep functions measured at waiting times t_w below 2400 s collapsed with an aging exponent μ of 0.4. Fitting all 1120 data points of Fig. 6 by a single power law gave a correlation coefficient $r^2=0.963$. Collapse of this kind is a typical feature of glassy systems that are aging.

materials that are aging [17,18]. Furthermore, for waiting times up to 2000 s, creep functions collapsed when plotted against a rescaled time t_μ, defined as $t_\mu=t/(t_w)^\mu$, with an aging exponent μ equal to 0.4 (Fig. 6). For waiting times above 2000 s, creep functions could be collapsed as well but the aging exponent was found to be greater than 1 (data not shown).

Similar experiments conducted with microbeads coated with acLDL showed no evidence of rejuvenation (Fig. 7, inset) or aging (Fig. 7). When submitted to a large oscillatory shear [stress history similar to Fig. 3(a)], the creep function $j_2(t)$ was not increased compared to $j_1(t)$ (Fig. 7, inset). When creep functions were measured following the large shear [stress history similar to Fig. 5(a)], no differences were noticed for waiting times below 2000 s (Fig. 7).

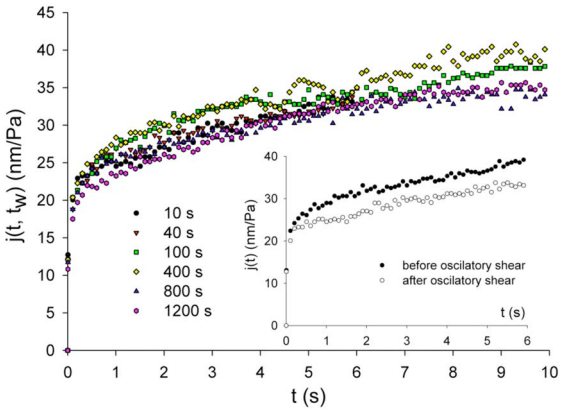

FIG. 7. (Color online) acLDL-coated microbeads did not show aging or rejuvenation ($n=613$ microbeads). Creep function measured at different waiting times t_w (from 10 to 1200 s) did not change with t_w, thus aging was not present. Inset: when applying a large oscillatory shear, rejuvenation was not present.

IV. DISCUSSION

We have measured material properties of the HASM cell before, during, and after application of a large oscillatory shear. Our principal findings are as follows. The complex modulus showed amplitude dependencies that were systematic but small. Shear softening was unveiled by transient application of a large oscillatory shear. Upon shear cessation, there was an immediate softening that was dependent on the duration of the applied shear and consistent with physical rejuvenation. This softening was followed by slow scale-free recovery of mechanical properties that was consistent with physical aging. Importantly, acLDL-coated microbeads, which do not connect to deep cytoskeletal structures, displayed neither physical aging nor rejuvenation.

In this section we first critique the methods used, and address in depth artifacts that might have been induced by the magnetic microbead approach. We then go on to discuss insights that these findings provide concerning material properties of the living cell, and their modifications induced by shear. Finally, we contrast the observed behaviors to those of inert soft glassy systems.

A. Methodological limitations

We have reported previously on optical magnetic twisting cytometry and its technical limitations [11,19,21,23]. Because data and interpretations reported here rest entirely upon that approach, we provide a critical summary of those methodological considerations. We begin by noting that the use of functionalized surface-bound probes to measure cytoskeletal mechanics has become a standard part of an armamentarium that now includes magnetic twisting cytometry, magnetic and optical tweezers, one-point and two-point microrheology, laser tracking microrheology, and even certain instances of atomic force microscopy [5,6,9,14,19,23,25–32]. Therefore the complex issue of coupling of a functionalized probe to the cell is not at all peculiar to OMTC.

In each of these techniques, the cell regards the probe as a part of its extracellular matrix. In the case of microbeads functionalized with RGD, binding between ligands on the microbead and integrin receptors on the cell surface induces the formation of focal adhesions. These focal adhesion complexes, in turn, connect to stress fibers and trigger a host of time-dependent responses that approximate those observed when a cell adheres to and spreads on a coated dish [33–36]. It is possible, nonetheless, that in all these methods results might be not so much a reflection of intrinsic properties of the CSK but instead attributable to the microbead-cell coupling, and especially, to the dynamics of receptor-ligand binding on the cell membrane. However, multiple lines of evidence argue against this possibility.

The structural and functional connections of the microbead to the CSK have been defined in a variety of experimental approaches [21,25,30,37–39], and mechanical responses measured in this way have been shown to be sensitive to manipulations of actin filaments, myosin motors, vinculin, heat shock proteins 20 and 27, cell spreading, cell stretching, cytoskeletal tension, and adenosine triphosphate (ATP) depletion [5,13,14,40–47]. These results are also in good agreement with a large number of studies that reported the effect of these and other drugs on cell mechanics but employed different measurement techniques, including indentation with a glass fiber [48], uniaxial stretching [49], atomic force microscopy [29,50], and measurement of the transit time of cells through capillary pores [51]. Importantly, since its discovery using OMTC [14], power law rheology has been widely confirmed using diverse experimental techniques, among which are optical tweezers [28,52], atomic force microscopy [29], uniaxial stretching [49], two-point microrheology [53], laser-tracking microrheology using surface-bound and internalized microbeads [27,31], and micropipette aspiration [54,55]. In every case, a power-law response with an exponent between 0.1 and 0.3 prevailed, implying that within the cell body relaxations at all time scales were present simultaneously; no distinct relaxation time stood out, and no distinct molecular relaxation time or time constant could characterize the response. Such a response is called scale-free.

But perhaps the strongest evidence pertaining to the issue of microbead-CSK coupling comes from a recent study that used OMTC to probe the freshly isolated airway smooth muscle cell. Deng and co-workers [56] demonstrated the existence of a high frequency regime in which the absolute magnitude and the frequency dependence of the complex modulus correspond precisely to entropic dynamics predicted for semiflexible actin filaments driven by thermal forces [57]. By establishing both qualitatively and quantitatively the hallmarks of entropic elasticity of a cross-linked actin network, these findings imply that the microbead response is dominated by actin filaments rather than integrin dynamics. Furthermore, using magnetic tweezers to pull on a microbead, Fenenberg and co-workers identified the rubber-like plateau of actin network in the nonlinear regime [58].

In connection with different microbead ligands, Puig-de-Morales and co-workers [21] investigated vitronectin, activating antibodies, and, importantly, nonactivating antibodies to different integrin subunits. As expected, mechanical moduli depended strongly on bead coating, differing at the extremes by as much as two orders of magnitude. But despite the differences in the signaling cascades that may be activated in each case, elastic and loss moduli increased with frequency f as a weak power law; therefore scale-free behavior prevailed and data collapsed onto the same universal relationships as did RGD-coated microbeads [23]. Thus scale-free rheology did not depend on the details of the coupling of the microbead to the cell.

As with all probes used to drive cell deformation, the resulting state of stress within the cell is complex [45,58,59]. In particular, Hu and co-workers used synchronous detection to show that strains applied through RGD-coated microbeads are transmitted to remarkable distances—approaching tens of micrometers—via stress fibers [45]. Moreover, using traction microscopy to measure the distribution of contractile stresses arising at the interface between a cell and its substrate, and using OMTC to measure g', Wang and co-workers showed a linear correlation between g' and the level of tensile stress within the CSK [46]. In addition, the power-law dependence upon frequency of cell stiffness measured by OMTC is pre-

dicted by traction microscopy measured at the cell base [44].

None of these observations is easily explained by ligation dynamics, and certainly not all of them. Rather these observations, taken together, support the simplest of all possible interpretations, namely, that the coupling of the microbead to the cell is stiff and that rheology reflects predominantly the mechanical nature of cytoskeletal structures. The physical picture, therefore, is that the microbead binds avidly to the cell, which in turn forms associated focal adhesions. And as the microbead rotates, the CSK is necessarily deformed. These deformations, in turn, are transmitted via stress fibers deeply into the cell body and down to basal adhesions attached at the cell substrate.

B. Amplitude dependence

In the literature, both linear and nonlinear behaviors have been reported [19,23,60,61]. Using methods and living cells similar to those used here, Fabry and co-workers reported that the storage modulus is independent of the torque amplitude [23], whereas Stamenovic and co-workers reported a slight dependence in the low range of torque amplitude [61]. Here we have reexamined the effects of torque amplitude in greater detail, and found amplitude dependencies that were systematic but quite weak. When the cells were relaxed, the response was perfectly linear. It is only when the cells were contacted that small nonlinearities appeared.

C. Rejuvenation

A large oscillatory shear was shown to induce significant softening of the CSK (Fig. 3). Similar shear softening has been reported in neutrophils subjected to mechanical shear [10,12]; those authors speculated that this softening might be attributable to disruption of bonds in the F-actin network and actin depolymerization.

Although mechanisms behind shear softening are still to be elucidated, the experiments reported here give interesting insights. During application of the large oscillatory shear, the stiffness of HASM cells remained nearly constant [Fig. 3(e)]. Therefore the decrease in stiffness seen upon shear cessation does not appear to be compatible with disruption of the F-actin network or with detachment of the microbead from focal adhesion complexes. The decrease in stiffness was virtually instantaneous and was tied to shear cessation. As such, the origin of this phenomenon appears to lie in the physical nature of the perturbation rather than intracellular signaling events that it might have triggered. Because shear softening was present when the cell was probed using RGD-coated microbeads (Fig. 3), but not present when probed using acLDL-coated microbeads (Fig. 7), the locus of the shear softening would appear to be the focal adhesion complex or the actin microfilament bundles and stress fibers.

Softening in response to stretch as reported here stands in contrast to reinforcement [4–9]. Reinforcement is a localized strengthening of cytoskeletal linkages induced by a restraining force applied on fibronectin-coated microbeads. In contrast, rejuvenation is a softening induced by a large shear applied on RGD-coated microbeads. Differences in experimental protocols and in cell type might explain this apparent contradiction. Choquet and co-workers begin measurements within seconds of microbead contact on the cell, thus focal adhesions are still not matured [6]. While focusing measurements upon lamellipodia of migrating fibroblasts, they observed directed, quasiballistic microbead motions, with microbead speeds of $5-10\ \mu$m/min. Moreover, Choquet and co-workers noticed that strengthening of cytoskeletal linkages was inhibited with phenylarsine oxide (PAO), a tyrosine phosphatase inhibitor, indicating a role for dephosphorylation. When PAO was added in our system (5 nM), we observed a twofold decrease in stiffness within 10 min of the drug application; the power law exponent dropped from 0.17 to 0.12, but rejuvenation and aging were still observed (data not shown). Finally, differences in focal adhesion constitution could explain the observed disparities. RPTPα and $\alpha_v\beta_3$ integrins are implicated in force sensing leading to reinforcement [9], but these two membrane proteins are found at the leading edge of lamellipodia of spreading cells [7]. In the experiments reported here, cells were grown at confluence, and RGD-coated microbeads were randomly distributed over the apical surface of the cell.

D. Evolution of mechanical properties

From our experiments, the following evolution of mechanical properties was unveiled. Up to an hour after microbead incubation and as long as no torque was applied to the microbeads, the stiffness remained constant; creep functions measured right after microbead incubation [Fig. 3(b)] and one hour later (Fig. 5) were not significantly different ($p=0.17$ using an unpaired two-tailed t test). When creep functions were regularly performed but no large shear was applied, the stiffness remained constant for the first 30 min and then began to increase strongly, as shown by Bursac and co-workers [13]. We were intrigued by this phenomenon, and, as such, we postponed measurements by 1 h after microbead incubation (Fig. 5). Surprisingly, we observed the very same behavior. Thus the strong increase in stiffness was directly linked to the beginning of measurements themselves; the small torque applied to measure the creep functions was responsible for the subsequent increase in stiffness. A similar stiffening has been previously reported [42,62,63] and was attributed to actin polymerization around the microbead. This increase in stiffness differed from that seen in reinforcement in that it was not inhibited by phenylarsine oxide (data not shown) and occurred on time scales of thousands of seconds rather than tens of seconds [6].

E. Cytoskeleton of the adherent living cell as a soft glassy material

Fabry and co-workers [14,23] were the first to point out the striking analogy between cell rheology and that of so-called soft glassy materials (SGMs). The class of SGMs includes foams, pastes, colloids, emulsions, and slurries; though very different in structure, the mechanical behavior of each is surprisingly alike. All are very soft (in the range of Pa to kPa), both the storage g' and the loss g'' moduli increase with weak power-law dependences on frequency, and the ratio g''/g' is frequency insensitive and in the order of

0.1 [16]. But while glassy systems tend to express scale-free rheology, all materials expressing scale-free rheology are not glassy; plastics, wood, concrete, and some metals fall into the latter category [24]. As such, the extent to which dynamics of the CSK might be regarded as being glassy remained very much an open question, and the search of unequivocal phenomena of soft condensed systems, such as physical aging and rejuvenation, becomes of great interest.

The similarities between the CSK of the living cell and soft condensed systems are striking. First, the elastic modulus of the living cell is of the order 10^2–10^4 Pa, showing that it is a very soft material indeed, and its loss tangent (or hysteresivity) is of the order 0.3, showing that it is much closer to being an elastic solid than a viscous fluid [14,23]. Second, a distinct internal time scale cannot characterize cell rheology. Instead, relaxation times are distributed as a power law, and for that reason cell rheology is said to be scale-free [14,19,23,27–29,49,52–54]. Third, the cell interior is characterized by molecular crowding, with an average distance between macromolecules of only 2 nm. Finally, out-of-equilibrium dynamics reported here showed strong similarities with rejuvenation (Figs. 3 and 4) and aging (Fig. 5) as observed in SGMs. Furthermore, collapse of mechanical measurements onto a master curve (Fig. 6), with an aging exponent of 0.4, is a typical feature of SGMs that are aging. As aging progresses, kinetics slow and the spectrum of mechanical relaxation times shifts downward with the waiting time, but at each t_w, the spectrum shape is unchanged [18]; thus using the rescaled time t_μ, mechanical measurements collapse onto a master curve [17]. Such a rescaling is a conventional method to prove aging and has been found in different SGMs, with aging exponents ranging from 0.55 to infinity [64–67].

If the soft glassy rheology model is applied to the CSK, then kinetic arrest becomes a key feature of cytoskeletal dynamics. As such, the following physical picture emerges [13]. A cytoskeletal element (presumably a structural protein or protein complex) finds itself trapped in an energy well, where trapping might arise from physical interactions such as molecular crowding, attractive interactions, or weak chemical bonding. Through a discrete molecular rearrangement, the CSK goes from one configuration to another, and evolves into configurations that are more and more stable, i.e., it ages. An externally applied mechanical strain provides an energy source that drives structural rearrangements, reverses aging, and pushes the CSK further away from thermodynamic equilibrium, i.e., the CSK is rejuvenated.

However, an interesting distinction between the CSK and inert condensed systems is the role played by the additional mechanical energy provided by ATP hydrolysis. ATP-dependent rearrangements of the CSK could modify the configurations themselves, providing an alternate means of exploring new configurations. ATP hydrolysis can drive both protein conformational changes and polymerization or depolymerization cycles, either of which could conceivably resolve constraints and drive structural rearrangements. This is radically different from traditional glassy systems that remain trapped in a configuration for increasingly long times because only thermal energy is available to allow the system to evolve [13].

The analogy between the CSK of the living cell and inert soft glassy systems, and the physical picture described above, bring together elastic energy storage, mechanical energy dissipation, and structural rearrangements within the living cell, thus tying together the abilities of the CSK to deform, to flow, and to remodel [11,13,68]. These factors determine the extent to which the material exhibits fluidlike versus solidlike behavior, and thus might impact understanding of those integrative cell functions that are dependent upon mechanical features. The analogy described here is purely empirical, however, and why the CSK should behave in a manner comparable to inert soft glassy systems remains unclear.

F. Rejuvenation and bronchospasm

To conclude, we turn to a more physiological problem, namely, how rejuvenation could help to understand bronchospasm. The mechanical environment of many living cells is dynamic; with every beat of the heart, inflation of the lung, or peristalsis of the gut, cells are often subjected to large mechanical strains. A deep inspiration, for example, is the most potent of all known bronchodilatory agencies, but this beneficial effect is abrogated in asthma, and the underlying mechanism remains unclear [69–74]. The potent bronchodilatory response to a deep inspiration has been attributed mainly to perturbed binding kinetics of myosin to actin; small cyclic stretches dramatically reduce the duty cycle of myosin [75,76]. It has been well recognized, however, that perturbed myosin binding by itself cannot provide an adequate explanation of this important phenomenon [77,78]. In response to stretch, airway smooth muscle demonstrates important cytoskeletal remodeling [79–81] and a time course of recovery of muscle properties that is anomalous. For example, after a transient stretch of the activated smooth muscle strip, or after a deep inspiration in a bronchoconstricted living human subject, the recovery of muscle force and muscle stiffness [76,77], as well as renarrowing of the airways [82], seem in some cases to be scale-free and are certainly far too slow to be accounted for by any straightforward accounting of myosin-actin binding dynamics [83]. We suggest, therefore, that myosin binding considered within the broader context of trapping, rejuvenation, aging, and associated slow glassy dynamics, might help to provide a more complete explanation of this basic bronchodilatory phenomenon.

ACKNOWLEDGMENTS

We thank Reynold A. Panettieri, Jr. for providing HASM cells, Stanley S. Hu for programming the OMTC, Emil Millet for producing magnetic microbeads, and Rebecca Stearns for scanning electron microscopy. We are grateful to Mark Coughlin for a careful reading of this manuscript. This study was supported by National Institute of Health Grants No. HL 33009, No. HL 65960, and No. HL 084224.

[1] D. E. Ingber, FASEB J. **20**, 811 (2006).
[2] P. A. Janmey and D. A. Weitz, Trends Biochem. Sci. **29**, 364 (2004).
[3] A. J. Engler, S. Sen, H. L. Sweeney, and D. E. Discher, Cell **126** 677 (2006).
[4] N. Rosenblatt, S. Hu, J. Chen, N. Wang, and D. Stamenovic, Biochem. Biophys. Res. Commun. **321**, 617 (2004).
[5] X. Trepat, M. Grabulosa, F. Puig, G. N. Maksym, D. Navajas, and R. Farre, Am. J. Physiol. Lung Cell Mol. Physiol. **287**, L1025 (2004).
[6] D. Choquet, D. P. Felsenfeld, and M. P. Sheetz, Cell **88**, 39 (1997).
[7] G. von Wichert, B. Haimovich, G. S. Feng, and M. P. Sheetz, EMBO J. **22**, 5023 (2003).
[8] C. G. Galbraith, K. M. Yamada, and M. P. Sheetz, J. Cell Biol. **159**, 695 (2002).
[9] G. Jiang, A. H. Huang, Y. Cai, M. Tanase, and M. P. Sheetz, Biophys. J. **90**, 1804 (2006).
[10] M. A. Tsai, R. S. Frank, and R. E. Waugh, Biophys. J. **65**, 2078 (1993).
[11] X. Trepat, L. Deng, S. S. An, D. Navajas, D. J. Tschumperlin, W. T. Gerthoffer, J. P. Butler, and J. J. Fredberg, Nature (London) **447**, 592 (2007).
[12] B. Yap and R. D. Kamm, J. Appl. Physiol. **98**, 1930 (2005).
[13] P. Bursac, G. Lenormand, B. Fabry, M. Oliver, D. A. Weitz, V. Viasnoff, J. P. Butler, and J. J. Fredberg, Nat. Mater. **4**, 557 (2005).
[14] B. Fabry, G. N. Maksym, J. P. Butler, M. Glogauer, D. Navajas, and J. J. Fredberg, Phys. Rev. Lett. **87**, 148102 (2001).
[15] E. R. Weeks, J. C. Crocker, A. C. Levitt, A. Schofield, and D. A. Weitz, Science **287**, 627 (2000).
[16] P. Sollich, Phys. Rev. E **58**, 738 (1998).
[17] L. C. E. Struick, *Physical Aging in Amorphous Polymers and Other Materials* (Elsevier, Houston, Texas, 1978).
[18] R. G. Larson, *The Structure and Rheology of Complex Fluids* (Oxford University Press, New York, Oxford, 1999), Vol. 1, p. 663.
[19] G. Lenormand, E. Millet, B. Fabry, J. P. Butler, and J. J. Fredberg, J. R. Soc., Interface **1**, 91 (2004).
[20] R. O. Hynes, Cell **110**, 673 (2002).
[21] M. Puig-de-Morales, E. Millet, B. Fabry, D. Navajas, N. Wang, J. P. Butler, and J. J. Fredberg, Am. J. Physiol.: Cell Physiol. **287**, C643 (2004).
[22] S. M. Mijailovich, M. Kojic, M. Zivkovic, B. Fabry, and J. J. Fredberg, J. Appl. Physiol. **93**, 1429 (2002).
[23] B. Fabry, G. N. Maksym, J. P. Butler, M. Glogauer, D. Navajas, N. A. Taback, E. J. Millet, and J. J. Fredberg, Phys. Rev. E **68**, 041914 (2003).
[24] W. N. Findley, J. S. Lai, and K. Onaran, *Creep and Relaxation of Nonlinear Viscoelastic Materials with an Introduction to Linear Viscoelasticity* (Dover Publications, Inc., Mineola, New York, 1989).
[25] D. R. Overby, B. D. Matthews, E. Alsberg, and D. E. Ingber, Acta Biomater. **1**, 295 (2005).
[26] B. A. Smith, H. Roy, P. De Koninck, P. Grutter, and Y. De Koninck, Biophys. J. **92**, 1419 (2007).
[27] S. Yamada, D. Wirtz, and S. C. Kuo, Biophys. J. **78**, 1736 (2000).
[28] M. Balland, A. Richert, and F. Gallet, Eur. Biophys. J. **34**, 255 (2005).
[29] J. Alcaraz, L. Buscemi, M. Grabulosa, X. Trepat, B. Fabry, R. Farre, and D. Navajas, Biophys. J. **84**, 2071 (2003).
[30] K. M. Van Citters, B. D. Hoffman, G. Massiera, and J. C. Crocker, Biophys. J. **91**, 3946 (2006).
[31] B. D. Hoffman, G. Massiera, K. M. Van Citters, and J. C. Crocker, Proc. Natl. Acad. Sci. U.S.A. **103**, 10259 (2006).
[32] A. R. Bausch, F. Ziemann, A. A. Boulbitch, K. Jacobson, and E. Sackmann, Biophys. J. **75**, 2038 (1998).
[33] J. Chen, B. Fabry, E. L. Schiffrin, and N. Wang, Am. J. Physiol.: Cell Physiol. **280**, C1475 (2001).
[34] C. J. Meyer, F. J. Alenghat, P. Rim, J. H. Fong, B. Fabry, and D. E. Ingber, Nat. Cell Biol. **2**, 666 (2000).
[35] G. Plopper and D. E. Ingber, Biochem. Biophys. Res. Commun. **193**, 571 (1993).
[36] C. E. Schmidt, A. F. Horwitz, D. A. Lauffenburger, and M. P. Sheetz, J. Cell Biol. **123**, 977 (1993).
[37] B. D. Matthews, D. R. Overby, F. J. Alenghat, J. Karavitis, Y. Numaguchi, P. G. Allen, and D. E. Ingber, Biochem. Biophys. Res. Commun. **313**, 758 (2004).
[38] N. J. Sniadecki, R. A. Desai, S. A. Ruiz, and C. S. Chen, Ann. Biomed. Eng. **34**, 59 (2006).
[39] N. Wang, J. P. Butler, and D. E. Ingber, Science **260**, 1124 (1993).
[40] S. S. An, B. Fabry, M. Mellema, P. Bursac, W. T. Gerthoffer, U. S. Kayyali, M. Gaestel, S. A. Shore, and J. J. Fredberg, J. Appl. Physiol. **96**, 1701 (2004).
[41] S. S. An, R. E. Laudadio, J. Lai, R. A. Rogers, and J. J. Fredberg, Am. J. Physiol.: Cell Physiol. **283**, C792 (2002).
[42] L. Deng, N. J. Fairbank, D. J. Cole, J. J. Fredberg, and G. N. Maksym, J. Appl. Physiol. **99**, 634 (2005).
[43] R. E. Laudadio, E. J. Millet, B. Fabry, S. S. An, J. P. Butler, and J. J. Fredberg, Am. J. Physiol.: Cell Physiol. **289**, C1388 (2005).
[44] D. Stamenovic, B. Suki, B. Fabry, N. Wang, and J. J. Fredberg, J. Appl. Physiol. **96**, 1600 (2004).
[45] S. Hu, J. Chen, B. Fabry, Y. Numaguchi, A. Gouldstone, D. E. Ingber, J. J. Fredberg, J. P. Butler, and N. Wang, Am. J. Physiol.: Cell Physiol. **285**, C1082 (2003).
[46] N. Wang, I. M. Tolic-Norrelykke, J. Chen, S. M. Mijailovich, J. P. Butler, J. J. Fredberg, and D. Stamenovic, Am. J. Physiol.: Cell Physiol. **282**, C606 (2002).
[47] R. M. Ezzell, W. H. Goldmann, N. Wang, N. Parasharama, and D. E. Ingber, Exp. Cell Res. **231**, 14 (1997).
[48] T. Wakatsuki, B. Schwab, N. C. Thompson, and E. L. Elson, J. Cell. Sci. **114**, 1025 (2001).
[49] N. Desprat, A. Richert, J. Simeon, and A. Asnacios, Biophys. J. **88**, 2224 (2005).
[50] C. Rotsch, F. Braet, E. Wisse, and M. Radmacher, Cell Biol. Int. **21**, 685 (1997).
[51] R. S. Frank, Blood **76**, 2606 (1990).
[52] M. Yanai, J. P. Butler, T. Suzuki, H. Sasaki, and H. Higuchi, Am. J. Physiol.: Cell Physiol. **287**, C603 (2004).
[53] A. W. C. Lau, B. D. Hoffmann, A. Davies, J. C. Crocker, and T. C. Lubensky, Phys. Rev. Lett. **91**, 198101 (2003).
[54] K. N. Dahl, A. J. Engler, J. D. Pajerowski, and D. E. Discher, Biophys. J. **89**, 2855 (2005).
[55] A. C. Rowat, J. Lammerding, and J. H. Ipsen, Biophys. J. **91**, 4649 (2006).
[56] L. Deng, X. Trepat, J. P. Butler, E. Millet, K. G. Morgan, D. A. Weitz, and J. Fredberg, Nat. Mater. **5**, 636 (2006).

[57] F. Gittes and F. C. MacKintosh, Phys. Rev. E **58**, R1241 (1998).
[58] W. Feneberg, M. Aepfelbacher, and E. Sackmann, Biophys. J. **87**, 1338 (2004).
[59] S. Hu, L. Eberhard, J. Chen, J. C. Love, J. P. Butler, J. J. Fredberg, G. M. Whitesides, and N. Wang, Am. J. Physiol.: Cell Physiol. **287**, C1184 (2004).
[60] J. Ohayon, P. Tracqui, R. Fodil, S. Fereol, V. M. Laurent, E. Planus, and D. Isabey, J. Biomech. Eng. **126**, 685 (2004).
[61] D. Stamenovic, Z. Liang, J. Chen, and N. Wang, J. Appl. Physiol. **92**, 1443 (2002).
[62] L. Deng, N. J. Fairbank, B. Fabry, P. G. Smith, and G. N. Maksym, Am. J. Physiol.: Cell Physiol. **287**, C440 (2004).
[63] P. G. Smith, L. Deng, J. J. Fredberg, and G. N. Maksym, Am. J. Physiol. Lung. Cell. Mol. Physiol. **285**, L456 (2003).
[64] C. Derec, G. Ducouret, A. Ajdari, and F. Lequeux, Phys. Rev. E **67**, 061403 (2003).
[65] L. Ramos and L. Cipelletti, Phys. Rev. Lett. **87**, 245503 (2001).
[66] M. Cloitre, R. Borrega, and L. Leibler, Phys. Rev. Lett. **85**, 4819 (2000).
[67] D. Bonn, S. Tanase, B. Abou, H. Tanaka, and J. Meunier, Phys. Rev. Lett. **89**, 015701 (2002).
[68] G. Lenormand and J. J. Fredberg, Biorheology **43**, 1 (2006).
[69] P. Malmberg, K. Larsson, B. M. Sundblad, and W. Zhiping, Eur. Respir. J. **6**, 680 (1993).
[70] A. Gump, L. Haughney, and J. Fredberg, J. Appl. Physiol. **90**, 2306 (2001).
[71] C. Y. Seow and J. J. Fredberg, J. Appl. Physiol. **91**, 938 (2001).
[72] J. E. Fish, M. G. Ankin, J. F. Kelly, and V. I. Peterman, J. Appl. Physiol. **50**, 1079 (1981).
[73] G. Skloot, S. Permutt, and A. Togias, J. Clin. Invest. **96**, 2393 (1995).
[74] J. J. Fredberg, J. Allergy Clin. Immunol. **106**, 615 (2000).
[75] S. J. Gunst, J. Appl. Physiol. **55**, 759 (1983).
[76] J. J. Fredberg, D. Inouye, B. Miller, M. Nathan, S. Jafari, S. H. Raboudi, J. P. Butler, and S. A. Shore, Am. J. Respir. Crit. Care Med. **156**, 1752 (1997).
[77] L. Wang, P. D. Pare, and C. Y. Seow, J. Appl. Physiol. **88**, 2246 (2000).
[78] G. G. King, P. D. Pare, and C. Y. Seow, Respir. Physiol. **118**, 1 (1999).
[79] L. E. Ford, C. Y. Seow, and V. R. Pratusevich, Can. J. Physiol. Pharmacol. **72**, 1320 (1994).
[80] S. J. Gunst and M. F. Wu, J. Appl. Physiol. **90**, 741 (2001).
[81] J. J. Fredberg, D. S. Inouye, S. M. Mijailovich, and J. P. Butler, Am. J. Respir. Crit. Care Med. **159**, 959 (1999).
[82] C. W. Thorpe, C. M. Salome, N. Berend, and G. G. King, J. Appl. Physiol. **97**, 1643 (2004).
[83] S. M. Mijailovich, J. P. Butler, and J. J. Fredberg, Biophys. J. **79**, 2667 (2000).